# The relationship between visual resolution and cone spacing in the human fovea

Ethan A Rossi[1] & Austin Roorda[1,2]

**Visual resolution decreases rapidly outside of the foveal center. The anatomical and physiological basis for this reduction is unclear. We used simultaneous adaptive optics imaging and psychophysical testing to measure cone spacing and resolution across the fovea, and found that resolution was limited by cone spacing only at the foveal center. Immediately outside of the center, resolution was worse than cone spacing predicted and better matched the sampling limit of midget retinal ganglion cells.**

Neural sampling of the retinal image is important for limiting human visual resolution at all locations in the visual field except for the fovea, where optical aberrations usually impose a fundamental limit[1–5]. When aberrations are minimized, the instantaneous postreceptoral information is believed to be limited by the spatial sampling of the cone photoreceptor mosaic in the fovea and possibly beyond[1–5]. To the first order, this limit can be considered to be the Nyquist sampling limit of the cone mosaic ($N_c$). Foveal cones each connect, via a cone bipolar cell, to at least two retinal ganglion cells (RGCs) and, as the majority of the RGCs in the central retina are of the midget class, it is presumed that each cone in the central fovea connects to both an ON- and OFF-center midget RGC (mRGC)[6,7]. This is the so-called 'private line' hypothesis[8], which forms the basis of the argument that cone spacing should limit resolution wherever this retinal circuitry is in place. At some point outside of the fovea, signals from multiple cones converge onto single mRGCs, compromising resolution, and thus, at some point, visual resolution no longer matches $N_c$, but instead matches the Nyquist limit of mRGCs[6,7].

The eccentricity where convergence in the mRGC network begins is not clear, with anatomical evidence suggesting that it begins between 3.5 and 6 degrees[6,7] from the foveal center. Psychophysical studies that sought to compare $N_c$ to visual resolution vary considerably, with estimates of the match between $N_c$ and resolution being anywhere between 2 and 10 degrees from the foveal center[1–5]. Consequently, the relationship between visual resolution and $N_c$ remains unknown (**Supplementary Discussion**). The large variability in psychophysical investigations stems, in part, from the difficulty in directly measuring both $N_c$ and optically optimal visual resolution in the same individual[3,5], forcing comparisons of their resolution measurements with sampling limits derived from different eyes, primarily from histological reports[1,2,4]. It is now well established that cone spacing, especially in the central fovea, is highly variable between individuals[9], making

these comparisons susceptible to error. The adaptive optics scanning laser ophthalmoscope[10] overcomes these limitations, allowing simultaneous measurement of the minimum angle of resolution (MAR), the cone spacing, and the precise location and motion of the stimulus across the retina.

An adaptive optics scanning laser ophthalmoscope was used to project an adaptive optics corrected tumbling E stimulus onto the retina at several locations in the central fovea (0–2.5° from the foveal center[8]) of five observers. Adaptive optics minimizes blur by measuring ocular aberrations and compensating for them with an adaptive element, improving optical quality for imaging and high-resolution stimulus delivery[10–12]. Adaptive optics substantially improves vision[11] and has been shown to reduce the MAR at the preferred retinal locus of fixation (PRLF) by ~33% in normal observers[12]. In a four-alternative forced-choice task, observers reported the orientation while fixating the stimulus or a peripheral target. Each observer was tested at retinal locations temporal to the PRLF; one observer (S4) was also tested at superior, inferior and nasal locations. A video of the retina was acquired on each trial, encoding the exact location of retinal stimulation (**Supplementary Videos 1** and **2**).

We overlaid retinal imagery with a topographic map of stimulated cones for observer S3 (**Fig. 1**). A map was generated for each observer by precisely determining each cone that interacted with the stimulus over the course of each trial (**Supplementary Methods** and **Supplementary Video 3**). We observed the expected falloff in MAR with increased distance from the PRLF (**Fig. 2a**). Fixational variability caused some test locations to deviate slightly from the horizontal meridian (**Fig. 1**; actual distances from the PRLF are shown in **Fig. 2**). The magnitude and rate of reduction in MAR matched the performance reported by studies that measured resolution across the fovea using high-contrast laser interference fringes[1,2] (**Supplementary Fig. 1** and **Discussion**). An important value to note is the $E_2$ value (the eccentricity in degrees at which the threshold doubles); the mean $E_2$ of the MAR ($E_{2m}$) for all observers was ~1.275° ($n = 5$).

We plotted the $N_c$ along the horizontal temporal retina (**Fig. 2b**). Where cones were well resolved, we measured center-to-center intercone distance (ICD) directly from identified cone centers and used it to calculate $N_c$, where $N_c = \frac{\sqrt{3}}{2} \times ICD$. This conversion is
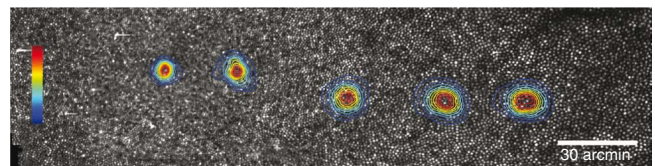


**Figure 1** Cone-stimulation map for subject S3. Cones appear as bright circles arranged in a triangular lattice pattern. Stimulated cones are shown as topographic maps overlaid in color. Color bar shows normalized level of cone stimulation.

[1]Vision Science Graduate Group and [2]School of Optometry, University of California, Berkeley, Berkeley, California, USA. Correspondence should be addressed to E.A.R. (earossi@berkeley.edu).

**Figure 2** Visual resolution matches the Nyquist limit of the mRGC mosaic but not the cone Nyquist limit. (**a**) Visual acuity as a function of eccentricity. Error bars are ± s.e.m. and are omitted where they are smaller than symbol. (**b**) Cone Nyquist limit across the horizontal temporal retina. Line colors match the symbol colors shown in the key (**d**). Solid lines are measurements and dashed lines are predictions. (**c**) Cone Nyquist limit and MAR for temporal test locations. Cone Nyquist limit is mean of cones in an elliptical area subtending ±2 s.d. of mean stimulated location. Error bars are ± s.e.m. and are omitted where they are smaller than symbol. The dashed black line is the 1:1 line. (**d**) Nyquist limit of mRGC and MAR. Only results along horizontal meridian are shown for S4. The dashed black line is the 1:1 line. For observer S4, t, n, s and i denote temporal, nasal, superior and inferior locations.



required because the Nyquist limit for a triangularly packed cone photoreceptor mosaic is based on the spacing between rows of cones[3]. An assessment of mosaic regularity confirmed that this was an appropriate method for calculating $N_c$ (**Supplementary Methods** and **Fig. 2**). Cones were resolved at the PRLF for one observer (S3); cones became resolved for other observers between 0.14–0.5° from the PRLF. We therefore estimated $N_c$ at the PRLF for these observers (and S2 at 0.4°) from retinal imagery (**Supplementary Methods**). Similar to $E_{2m}$, we were able to compute $E_{2c}$, the value at which $N_c$ doubles; the mean $E_{2c}$ was ~2.224° ($n = 5$), nearly twice the $E_{2m}$.

The measured MAR values were similar to estimates of $N_c$ at the PRLF (**Fig. 2c**), which is consistent with previous studies[1–5]. However, MAR decreased at a greater rate with increasing eccentricity than was predicted by $N_c$. If MAR exactly matched $N_c$, data points would be expected to fall on a 1:1 line. The slope is the important factor in this comparison, as a slope of 1 indicates that MAR is governed by $N_c$. A linear regression line was fit to the data of each observer independently. The mean slope was 0.6355 (s.d. = 0.1058, $n = 5$). This value was significantly different from 1 ($t$ test, one sample, $P = 0.00153$), indicating that MAR was worse than predicted by $N_c$ at locations eccentric to the PRLF. Choosing a different threshold for acuity (that is, 75% versus 82.5%) would only have resulted in horizontal translations of the regression line fits. Choosing a different metric to represent $N_c$ would have changed the slope; for the most extreme case of a square mosaic, the slope would still only have been ~0.73. Bland-Altman analysis[13] confirmed the poor agreement between MAR and $N_c$ across test locations (**Supplementary Fig. 3**). This discrepancy does not seem to be explainable by the nature of the stimulus (**Supplementary Discussion**) or task, as the tumbling E task has been shown to be a sampling limited task[14].

The area where visual resolution most closely matched $N_c$ (0–0.5°) corresponded well with the anatomically distinct foveola, the nearly flat floor of the foveal pit[8]. This retinal area has several features that are seemingly optimal for high spatial resolution, including maximum cone density, elongated waveguides, an absence of rods and S cones, and a lack of overlying vasculature and nerves[8,9]. However, we believe that the discord between resolution and $N_c$ seen outside the foveola was primarily a result of differences in retinal circuitry across the fovea. Because the fibers of Henle displace RGCs from the photoreceptors of the central retina to which they form connections, foveal circuitry has historically been difficult to characterize[6–8,15]. Careful study of these fibers leads to new predictions of mRGC receptive field density across the visual field[15]. Using a theoretical model of mRGC receptive field density[15], we estimated the Nyquist limit of the mRGC mosaic (the spacing between neighboring ON- or OFF-center mRGC receptive fields) at the resolution test locations along the horizontal meridian (**Supplementary Methods**) and compared it with the measured MAR (**Fig. 2d**). An individual regression line was fit for each observer. The mean slope was 1.0111 (s.d. = 0.1105, $n = 5$)
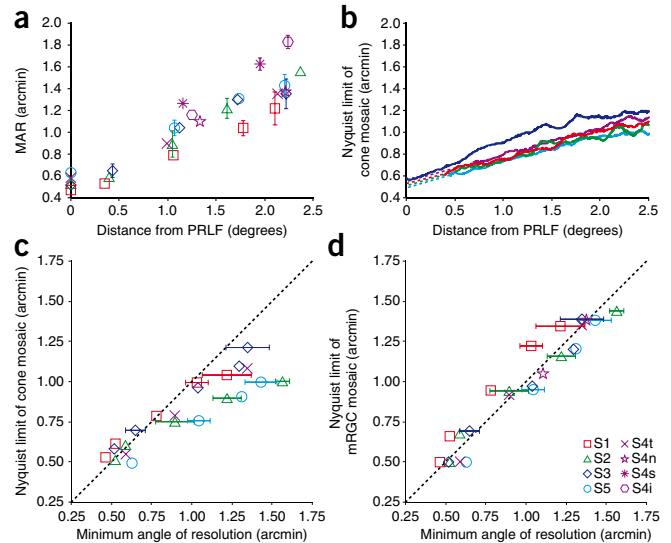
and this value did not differ significantly from 1 ($t$ test, one sample, $P = 0.8333$), indicating that MAR for this task is governed by the Nyquist limit of the mRGC mosaic across the fovea. Cortical mechanisms ultimately utilize the information provided by the earliest stages of visual processing in the retina to make a decision in a visual resolution task; that those decisions so closely match the theoretical sampling limits imposed by the first stages of retinal processing is notable.

*Note: Supplementary information is available on the Nature Neuroscience website.*

**AUTHOR CONTRIBUTIONS**
E.A.R. designed and performed the experiments, analyzed the data, and wrote the manuscript. A.R. supervised the project and edited the manuscript.

**COMPETING INTERESTS STATEMENT**
The authors declare competing financial interests: details accompany the full-text HTML version of the paper at http://www.nature.com/natureneuroscience/.

Published online at http://www.nature.com/natureneuroscience/.
Reprints and permissions information is available online at http://npg.nature.com/reprintsandpermissions/.

1. Green, D.G. *J. Physiol. (Lond.)* **207**, 351–356 (1970).
2. Enoch, J.M. & Hope, G.M. *Doc. Ophthalmol.* **34**, 143–156 (1973).
3. Williams, D.R. & Coletta, N.J. *J. Opt. Soc. Am. A* **4**, 1514–1523 (1987).
4. Thibos, L.N., Cheney, F.E. & Walsh, D.J. *J. Opt. Soc. Am. A* **4**, 1524–1529 (1987).
5. Marcos, S. & Navarro, R. *J. Opt. Soc. Am. A Opt. Image Sci. Vis.* **14**, 731–740 (1997).
6. Curcio, C.A. & Allen, K.A. *J. Comp. Neurol.* **300**, 5–25 (1990).
7. Dacey, D.M. *J. Neurosci.* **13**, 5334–5355 (1993).
8. Polyak, S.L. *The Retina* (University of Chicago Press, Chicago, 1941).
9. Curcio, C.A., Sloan, K.R., Kalina, R.E. & Hendrickson, A.E. *J. Comp. Neurol.* **292**, 497–523 (1990).
10. Roorda, A. *et al. Opt. Express* **10**, 405–412 (2002).
11. Liang, J., Williams, D.R. & Miller, D.T. *J. Opt. Soc. Am. A Opt. Image Sci. Vis.* **14**, 2884–2892 (1997).
12. Rossi, E.A., Weiser, P., Tarrant, J. & Roorda, A. *J. Vis.* **7**, 1–14 (2007).
13. Bland, J.M. & Altman, D.G. *Lancet* **1**, 307–310 (1986).
14. Anderson, R.S. & Thibos, L.N. *J. Opt. Soc. Am. A Opt. Image Sci. Vis.* **16**, 2334–2342 (1999).
15. Drasdo, N., Millican, C.L., Katholi, C.R. & Curcio, C.A. *Vision Res.* **47**, 2901–2911 (2007).